IEEE Access
Multidisciplinary | Rapid Review | Open Access Journal

Received May 22, 2020, accepted June 7, 2020, date of publication June 16, 2020, date of current version June 29, 2020.

Digital Object Identifier 10.1109/ACCESS.2020.3002789

Small Frequency Ratio Multi-Band Dielectric Resonator Antenna Utilizing Vertical Metallic Strip Pairs Feeding Structure

ASMAA I. AFIFI[1,2], (Student Member, IEEE), ADEL B. ABDEL-RAHMAN[1,3], ANWER S. ABD EL-HAMEED[2,4], (Member, IEEE), AHMED ALLAM[1], AND SABAH M. AHMED[5]

[1]Department of Electronics and Communications Engineering, Egypt-Japan University of Science and Technology, Alexandria 21934, Egypt
[2]Electronics Research Institute, Giza 12622, Egypt
[3]Electrical Engineering Department, Faculty of Engineering, South Valley University, Qena 83523, Egypt
[4]Center for Northeast Asian Studies, Tohoku University, Sendai 980-8576, Japan
[5]Department of Mechatronics and Robotics Engineering, Egypt-Japan University of Science and Technology, Alexandria 21934, Egypt

Corresponding author: Asmaa I. Afifi (asmaa.afifi@ejust.edu.eg)

This work was supported in part by the Egyptian Ministry of Higher Education, and in part by the Egypt-Japan University of Science and Technology, Egypt.

ABSTRACT In this study a quintuple band rectangular dielectric resonator antenna (RDRA) with a small frequency ratio and small size of 30 mm × 30 mm × 9.813 mm is introduced. The proposed RDRA covers the frequency bands of WLAN (2.4/5.2 GHz), WiMAX (3.5 GHz) and 5G (4.1/4.8 GHz) exploiting TE^{y}_{10}, TE^{x}_{211}, $TE^{y}_{1\delta1}$, TE^{y}_{111}, and $TE^{y}_{2\delta1}$ modes, respectively. A rectangular slot aperture is optimized to serve as a resonator with resonance mode TE^{y}_{10} as well as to couple the electric field from microstrip line to the DRA to excite TE^{x}_{211} mode. Furthermore, a new feeding approach employing three vertical metallic strip pairs (VMSPs) is proposed to excite further $TE^{y}_{1\delta1}$, TE^{y}_{111}, and $TE^{y}_{2\delta1}$ modes in the RDRA. The VMSPs are configured on both sides of the dielectric resonator (DR) along the y – direction to act as vertical electric current sources. The lengths, width, and positions of the VMSPs are carefully determined in order to attain the desired modes. The four RDRA modes have broadside patterns while the slot resonator mode has a pattern like a dipole. Good agreement between both measured and simulated results of the reflection coefficient, radiation pattern, and the gain is achieved.

INDEX TERMS Aperture, modes, RDRA, VMSPs, WiMAX, WLAN, wireless communications.

I. INTRODUCTION

With the development of the wireless communication during the last decades, the demand for the multiband antennas has increased [1]. Since a variety of the wireless applications such as WLAN, WiMAX, and 5G, designing single radiating element supports different applications is indispensable. The 5G wireless communication is more attractive than the 4G system due to its lower latency and high data rate with expanding wireless data traffic [2]. The 5G operating bands are yet to be determined exactly, but according to [3], [4], the 5G system will support both the lower (sub 6 GHz) and upper (millimeter wave) bands for better propagation and high data rate, respectively. Various wideband antennas that cover the WLAN, WiMAX bands as well as the lower 5G band have been reported [5]. However, these antennas have unwanted bands that cause noise. Multiband antenna can overcome this problem by selecting only the desired bands. Subsequently, the multiband planar and DRAs have received much attention in wireless applications. Dielectric resonator antennas introduce many advantages over the planar structure such as small size, low cost, and high efficiency due to the lack of surface wave and ohmic loss [6], [7].

Several techniques have been investigated to design multiband DRAs, such as stacked DRAs [8], multiple DRAs [9], hybrid DRAs [10], [19], using the feeding structure to add another band [11] and generation higher order modes [12]–[18]. However, most of these DRAs support either dual band [8]–[17], or high frequency ratio [19]. Although [12] and [18] achieve multiband with small

The associate editor coordinating the review of this manuscript and approving it for publication was Giovanni Angiulli.

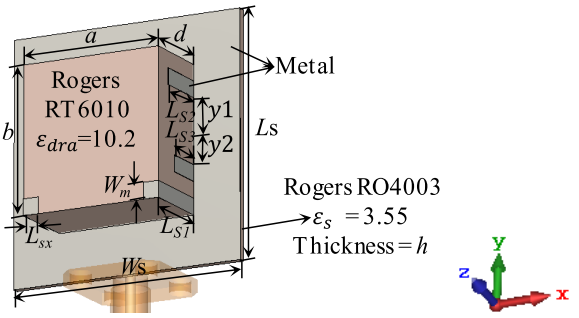

FIGURE 1. Geometry of the proposed multiband rectangular dielectric resonator antenna.

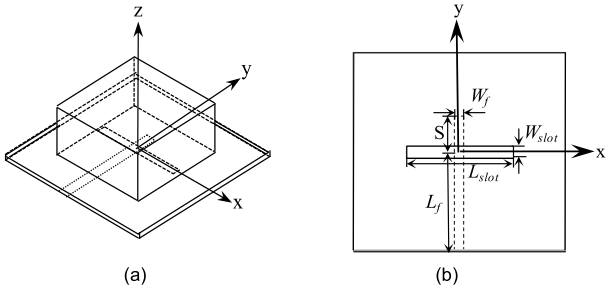

FIGURE 2. The proposed antenna without VMSPs. (a) 3D view. (b) Top view.

frequency ratio, the antenna size is obviously large corresponding to its lowest operating band.

In this paper, a design of compact small frequency ratio quintuple band RDRA is presented. The proposed antenna allows formation of five modes of TE^{y}_{10}, TE^{x}_{211} $TE^{y}_{1\delta1}$, TE^{y}_{111}, and $TE^{y}_{2\delta1}$ corresponding to 2.4/5.2 GHz WLAN, 3.5 GHz WiMAX, and 4.1/4.8 GHz 5G applications, respectively. In order to excite the five modes, three VMSPs are utilized as well as rectangular aperture feeding; VMSPs are to create three bands while a rectangular aperture is to generate one band and excite another. The introduced antenna of a small size of 30 mm×30 mm×9.813 mm exhibits good impedance matching, radiation patterns and gain across all operating bands. Through this paper, simulations have been carried out by CSTMWS and verified by the measurements. To the best of our knowledge, no researches were reported fulfilling these small frequency ratio operating bands with such compact size so far.

II. ANTENNA DESIGN

Fig.1 shows the geometry of the prospective multiband rectangular DRA excited by the aperture coupling feed as well as three VMSPs. The feeding aperture is engraved as a rectangular slot with dimensions of ($L_{slot} \times W_{slot}$) on the top side in the ground plane. A microstrip line of dimensions ($L_f \times W_f$) is loaded by open stub of length S and allocated on the back side of the dielectric substrate for feeding. Three VMSPs are settled on both sides of the DRA along the y-axis for multiband excitation purposes. Each VMSP is carefully designed to excite individual mode. A Rogers RT6010 dielectric material with relative permittivity $\varepsilon_{dra} = 10.2$ and loss tangent tan $\delta = 0.0023$ is selected to construct the DRA of length $a = 18$ mm, width $b = 18$ mm, and height $d = 9$ mm. The DR is supported by Rogers RO4003 substrate of dimensions $L_s \times W_s \times h = 30$ mm $\times$ 30 mm $\times$ 0.813 mm and a relative permittivity $\varepsilon_s = 3.55$.

A. APERTURE FEEDING APPROACH

In the aperture feeding scheme, the excited mode in the RDRA can be controlled by the direction and position of the slot. Referring to the DRA and coordinate system shown in Fig.2, the excited mode is TE^{x}, because the slot length is in x-direction. The field components inside the resonator can be represented as [20]:

$$E_x = 0 \tag{1}$$
$$E_y = Ak_z \cos(k_x x)\cos(k_y y)\sin(k_z z) \tag{2}$$
$$E_z = -Ak_y \cos(k_x x)\sin(k_y y)\cos(k_z z) \tag{3}$$
$$H_x = A\frac{k_y^2 + k_z^2}{j\omega\mu_0}\cos(k_x x)\cos(k_y y)\cos(k_z z) \tag{4}$$
$$H_y = A\frac{k_x k_y}{j\omega\mu_0}\sin(k_x x)\sin(k_y y)\cos(k_z z) \tag{5}$$
$$H_z = A\frac{k_x k_z}{j\omega\mu_0}\sin(k_x x)\cos(k_y y)\sin(k_z z) \tag{6}$$

where A is an arbitrary constant and the wavenumbers k_x, k_y, and k_z along the x, y, and z-directions inside the DR are obtained as follow [6],

$$k_x = \frac{n\pi}{a}, \quad k_y = \frac{m\pi}{b}, \text{ and } k_z = \frac{p\pi}{2d}$$

The wave numbers satisfy the following characteristic equation:

$$k_x^2 + k_y^2 + k_z^2 = \mu_{r,dra}\varepsilon_{r,dra}k_0^2 \tag{7}$$

where k_0 is the free space wavenumber, $\mu_{r,dra}$ and $\varepsilon_{r,dra}$ are the relative permeability and relative permittivity of the DRA. The dimensions of the proposed RDRA are using equation (7).

The modes of the proposed RDRA can be calculated by (8).

$$f_{mnp} = \frac{c}{2\pi\sqrt{\mu_{r,dra}\varepsilon_{r,dra}}}\sqrt{(\frac{n\pi}{a})^2 + (\frac{m\pi}{b})^2 + (\frac{p\pi}{2d})^2} \tag{8}$$

where $c = 3 \times 10^8$ m/s, $\varepsilon_{r,dra} = 10.2$, $\mu_{r,dra} = 1$, $a = 18$ mm, $b = 18$mm and $d = 9$mm.

Accordingly, to excite TE^{x}_{111} mode which will alter to the intended TE^{x}_{211} mode due to VMSPs effect as will be discussed later, the slot should be located near the maximum magnetic field in the RDRA. This condition is realized by (4), which indicate that for TE^{x}_{111} mode, the H_x component is maximum at $y = 0$ and $z = 0$. Therefore, the TE^{x}_{111} mode of 4.6 GHz is generated by keeping the slot at center of both ground and DRA as shown in Fig.2. To improve the coupling between the microstrip line and the slot, the open stub length should be integer multiples of a quarter guided wavelength [6].

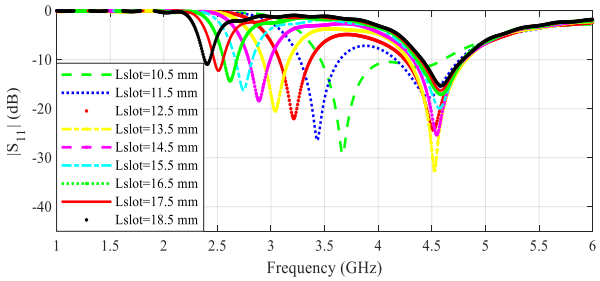

FIGURE 3. The antenna reflection coefficient in terms of the slot length (L_{slot}).

TABLE 1. Antenna geometrical parameters (unit: mm).

W_s	L_s	W_f	L_f	W_{slot}	L_{slot}	W_m	S	a
30	30	2	15.8	1.5	17.5	2	3	18
b	d	h	L_{S1}	L_{S2}	L_{S3}	L_{sx}	y_1	y_2
18	9	0.813	9	6.5	5	2	5	3

To generate another operating band at 2.5 GHz, the slot is exploited to act as a resonator with TE^y_{10} mode as well as its main function of DRA excitation. The slot resonance occurs approximately at $(\lambda_g/2)$ where $(\lambda_g = \frac{\lambda_0}{\sqrt{\varepsilon_{eff}\,\mu_{eff}}})$ denotes the guided wavelength inside the materials. In this case, the DR is considered as a load for the slot. The effective permittivity at the slot interface can be calculated as [21],

$$\varepsilon_{eff} = \frac{H_{total}}{h_d/\varepsilon_{dra} + h/\varepsilon_s} \tag{9}$$

where H_{total} is the total height of the antenna structure, h_d is the height of the DRA of permittivity ε_{dra}, and h is the substrate thickness of permittivity ε_s. Eventually, two important parameters can control the slot resonance frequency; slot length and the effective permittivity of both substrate and dielectric resonator.

To verify both functions of the slot, the reflection coefficient for different slot lengths are shown in Fig.3. It is indicated that the length of the slot controls the lower band while affecting the 4.6 GHz band matching. The slot length of $L_{slot} = 17.5$ mm is selected which correspond to 2.5 GHz WLAN band while keeping exciting the 4.6 GHz band of the TE^x_{111} mode. The optimized dimensions of the proposed RDRA are listed in Table 1. Furthermore, the open stub length effect is also studied in Fig.4 showing best matching for both bands at length $S = 3$mm.

B. VMSPs EXCITATION APPROACH

To utilize the DRA in generating extra modes, VMSPs are placed along y – direction at $|x| = a/2$ in both DRA sides and shortened to the ground to act as vertical electric sources as shown in Fig.1. Since the electric field in the slot, $E_a\hat{y}$ and the resulting equivalent magnetic current source $(\vec{M} = -\hat{z}XE_a\hat{y})$ must vanish at the ends of the slot due to the boundary condition on tangential components of the electric field. The current, $\vec{J}$ on the ground plane does the opposite, reaching its

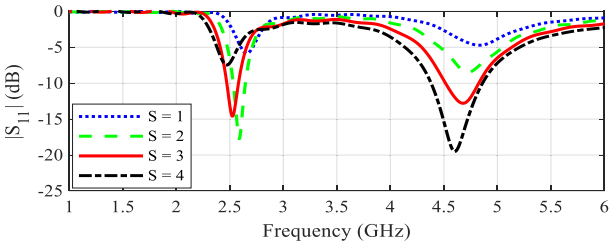

FIGURE 4. Reflection coefficient of the antenna without metallic strips in terms of the stub length(S).

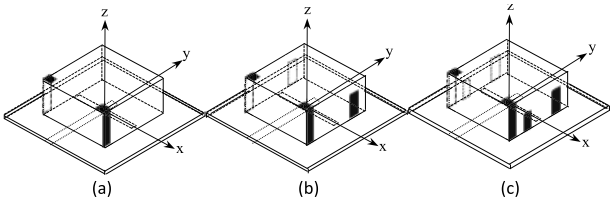

FIGURE 5. Geometry of various antennas used in the design procedure, (a) One VMSP, (b) Two VMSPs and (c) Three VMSPs (Proposed antenna).

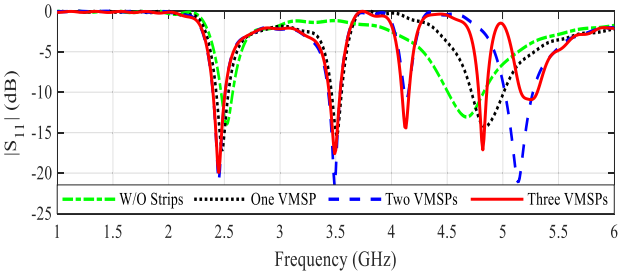

FIGURE 6. Effect of adding VMSPs on the reflection coefficient.

maximum around the edges of the slot and going to zero in the middle, therefore, the appropriate location of VMSPs to act as vertical electric source is at $|x| = a/2$ along y - direction. Due to symmetry, each VMSP has equal amplitude and in-phase RF signal at $|x| = a/2$. A. Petosa [6], proved that the vertical electric current sources generates TE^y_{mnp} modes. The electric field in z-direction for TE^y_{mnp} can be expressed by (10), which emphasis that the electric field is maximum at $|x| = a/2$.

$$E_z = Ak_x \sin(k_x x)\sin(k_y y)\cos(k_z z) \tag{10}$$

As a result, to excite $TE^y_{1\delta1}$, TE^y_{111}, and $TE^y_{2\delta1}$ modes which are corresponding to 3.5 GHz, 4.1 GHz, and 4.8 GHz respectively, three VMSPs are placed at $|x| = a/2$ along y - direction, while the height and position of each VMSP control the excited mode as detailed in [22]. The height and position of each VMSP are optimized to alter the E-field distribution inside the DR to excite each corresponding mode. Accordingly, to increase the electrical length of the longer VMSP in order to tune at 3.5 GHz, the corresponding VMSP has been bended above the top surface with length L_{sx}. The effect of strip width is minor compared to the strip height, so, the three VMSPs width are optimized to $W_m = 2$ mm to avoid inter-overlapping.

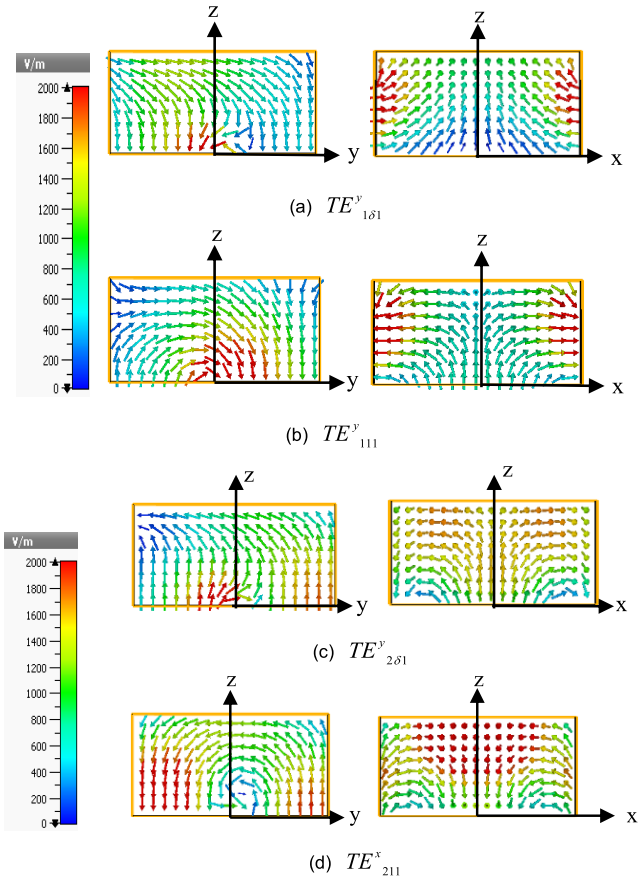

FIGURE 7. Simulated E-field distribution inside the proposed RDRA in both *yoz* and *xoz*-planes at, (a) 3.5 GHz. (b) 4.1 GHz. (c) 4.8 GHz. (d) 5.2 GHz.

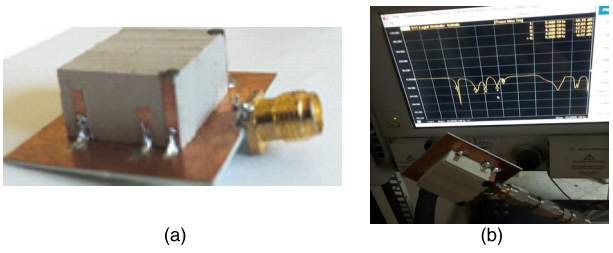

FIGURE 8. Fabrication of the proposed quintuple-band RDRA. (a) 3D view and (b) Measurement setup.

To track the effect of each VMSP, a set of simulations are carried out for four different cases; without VMSPs, with one VMSP, with two VMSPs, and with three VMSPs as shown in Fig.5. It is worth mentioning that the possibility of adding extra resonance peaks is still existing by adding extra VMSPs. The reflection coefficients of all cases are presented in Fig.6. It is noted that by adding the second VMSP, the frequency band of 4.6 GHz of the TE^{x}_{111} mode which is generated by aperture coupling is shifted to the desired WLAN frequency of 5.2 GHz of the TE^{x}_{211} mode. For more clarification, the electric field distributions of all excited modes are introduced in Fig.7. As shown in Fig.7(a),(b), the $TE^{y}_{1\delta 1}$ and TE^{y}_{111} have half wavelength field variation in both x and

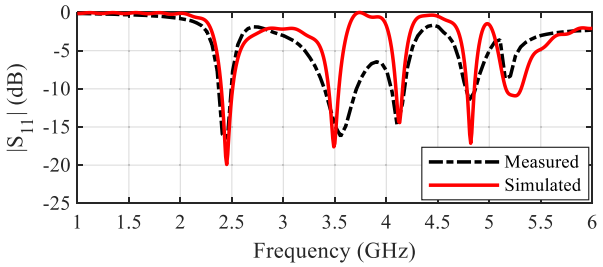

FIGURE 9. Simulated and measured reflection coefficient of the quintuple-band RDRA.

TABLE 2. Simulated and measured radiation efficiency of the proposed multiband antenna.

Antenna Parameter		Freq. (GHz) 2.4	3.5	4.1	4.8	5.2
Rad. Eff. (%)	Sim.	92.34	93.56	80	72.2	93.3
	Meas.	87.09	88.06	76.7	66.7	87.9

TABLE 3. Performance comparison of the proposed RDRA with other multiband antennas.

Ref	Number of Bands	DR Size (λ_g^3)	Frequency Ratio	Impedance Width (MHz)
[12]	Quintuple	1.76	1.478/1.23/1.1 /1.11	1950/270/590/ 950/870
[13]	Dual	0.554	1.46	61/30
[17]	Dual	0.362	1.23	147/132
[18]	Quad	0.179	1.25/ 1.6/1.042	230/200/590/ 200
[19]	Triple	0.044	2/1.3	39.6/227.88/ 68.77
This work	Quintuple	0.044	1.458/1.17/ 1.17/1.08	150/360/150/ 150/55

z-directions, while in y-direction, they have a fraction of half wavelength (which is indicated by δ) and one half wavelength field variation, respectively. Regarding the $TE^{y}_{2\delta 1}$ and TE^{x}_{211}, the field variation is two and one half wavelength in x and z-directions, respectively, but in y-direction, it is δ and one half wavelength, respectively as shown in Fig.7(c),(d).

III. MEASURMENT RESULTS

The presented multiband antenna was fabricated by using multiple layers of Rogers RT6010 material with $\varepsilon_{\text{dra}} = 10.2$ as shown in Fig.8. The simulated and measured reflection coefficients are shown in Fig.9, showing relatively good impedance matching over the five frequencies (2.4/3.5/4.1/4.8/5.2 GHz) with impedance bandwidths (150/360/150/50/55 MHz), respectively.

The slight variation between the measured and simulated reflection coefficient, particularly at 5.2 GHz is due to many factors: fabrication tolerance, manual assembling of multiple Rogers layers to construct the DR, and soldering effect of the SMA connector which was not taken into account during the simulation process. Fig.10 illustrates the measured and

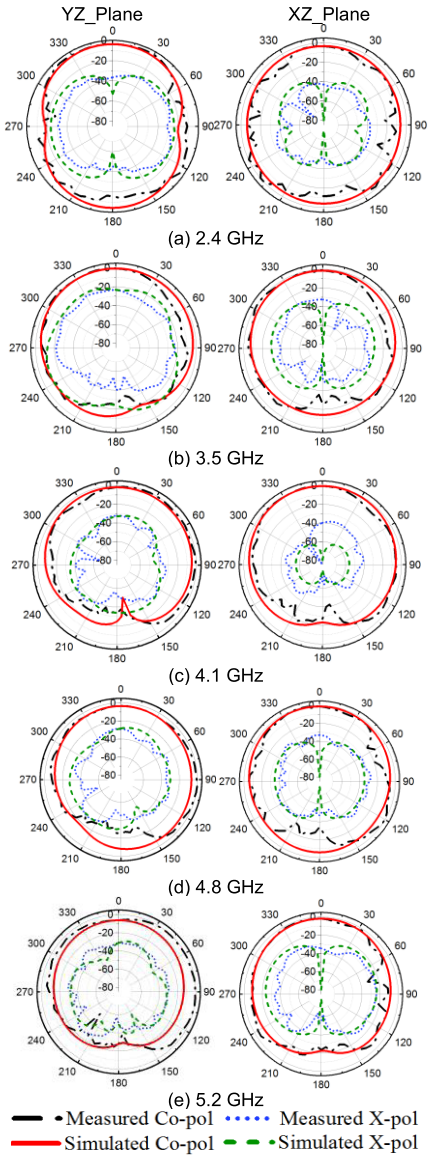

FIGURE 10. Measured and simulated radiation pattern of the proposed RDRA.

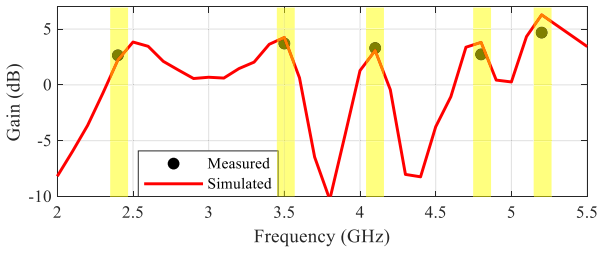

FIGURE 11. Measured and simulated gain of the proposed multi-band RDRA.

simulated radiation pattern of the introduced antenna at 2.4 GHz, 3.5 GHz, 4.1 GHz, 4.8 GHz, and 5.2 GHz, respectively. As expected, the four bands of the RDRA have broadside patterns, and the slot band has a pattern like a dipole. The measured and simulated gain of the proposed RDRA are compared in Fig.11. The figure shows that the fabricated prototype provides a good measured gain of 2.65 dBi, 3.7 dBi, 3.3 dBi, 2.73 dBi, and 4.68 dBi at 2.4 GHz, 3.5 GHz, 4.1 GHz, 4.8 GHz, and 5.2 GHz, respectively. The simulated and measured antenna radiation efficiency has been illustrated in Table 2. The simulated and measured antenna radiation efficiencies show satisfactory values at the interested bands. Finally, the designed RDRA performance was compared with the state-of-the-art designs as shown in Table 3. In order to have fair comparison, the DR size is presented compared to λ_g^3, where λ_g is calculated at the lowest frequency. The comparison shows that our structure has the smallest size that achieves quintuple bands with such small frequency ratio.

IV. CONCLUSION

A multiband RDRA is presented for WLAN, WiMAX, and 5G applications. A rectangular slot aperture is optimized to serve as resonator with resonance mode TE^y_{10}, as well as to couple the electric field to DRA to excite TE^x_{211} mode. Three VMSPs with different lengths are engaged at both sides of the DR along the $y-axis$ to excite three extra modes. The use of this technique is introduced to excite adjacent modes with a small frequency ratio. The presented antenna has a compact size of $0.135\lambda_g^3$, λ_g is the guided wavelength through the DR at the lowest band of 2.4 GHz. The suggested antenna was fabricated showing reasonable agreement between simulated and fabricated results. Gains of 2.65 dBi, 3.7 dBi, 3.3 dBi, 2.73 dBi, and 4.68 dBi are achieved corresponding to 2.4 GHz, 3.5 GHz, 4.1 GHz, 4.8 GHz, and 5.2 GHz, respectively.

REFERENCES

[1] D. A. Sanchez-Hernandez, *Multiband Integrated Antennas for 4G Terminals*. Norwood, MA, USA: Artech House, 2008.
[2] J. G. Andrews, S. Buzzi, W. Choi, S. Hanly, A. Lozano, A. Soong, and C. Zhang, "What will 5G be?" *IEEE J. Sel. Areas Commun.*, vol. 32, no. 6, pp. 1065–1082, Jun. 2014.
[3] *5G Spectrum Recommendations*, 5G Americas, Bellevue, WA, USA, Apr. 2017.
[4] *5G Spectrum Public Policy Position*, GSM Assoc., London, U.K., Jul. 2019.
[5] W. S. Yeoh and W. S. T. Rowe, "An UWB conical monopole antenna for multiservice wireless applications," *IEEE Antennas Wireless Propag. Lett.*, vol. 14, pp. 1085–1088, Jan. 2015.
[6] A. Petosa, *Dielectric Resonator Antenna Handbook*. Boston, MA, USA: Artech House, 2007.
[7] K. W. Leung, E. H. Lim, and X. S. Fang, "Dielectric resonator antennas: From the basic to the aesthetic," *Proc. IEEE*, vol. 100, no. 7, pp. 2181–2193, Jul. 2012.
[8] R. Khan, J. U. R. Kazim, M. H. Jamaluddin, O. Owais, and J. Nasir, "Multiband-dielectric resonator antenna for LTE application," *IET Microw., Antennas Propag.*, vol. 10, no. 6, pp. 595–598, Apr. 2016.
[9] M. S. Sharawi, S. K. Podilchak, M. U. Khan, and Y. M. Antar, "Dual-frequency DRA-based MIMO antenna system for wireless access points," *IET Microw., Antennas Propag.*, vol. 11, no. 8, pp. 1174–1182, Jun. 2017.
[10] Y. M. Pan, S. Y. Zheng, and W. Li, "Dual-band and dual-sense omnidirectional circularly polarized antenna," *IEEE Antennas Wireless Propag. Lett.*, vol. 13, pp. 706–709, Apr. 2014.
[11] H.-M. Chen, Y.-K. Wang, Y.-F. Lin, S.-C. Lin, and S.-C. Pan, "A compact dual-band dielectric resonator antenna using a parasitic slot," *IEEE Antennas Wireless Propag. Lett.*, vol. 8, pp. 173–176, Jun. 2009.
[12] G. Varshney, S. Gotra, V. S. Pandey, and R. S. Yaduvanshi, "Inverted-sigmoid shaped multiband dielectric resonator antenna with dual-band circular polarization," *IEEE Trans. Antennas Propag.*, vol. 66, no. 4, pp. 2067–2072, Apr. 2018.

[13] H. Tang, J.-X. Chen, W.-W. Yang, L.-H. Zhou, and W. Li, "Differential dual-band dual-polarized dielectric resonator antenna," *IEEE Trans. Antennas Propag.*, vol. 65, no. 2, pp. 855–860, Feb. 2017.
[14] D. Guha, P. Gupta, and C. Kumar, "Dualband cylindrical dielectric resonator antenna employing $HEM_{11\delta}$ and $HEM_{12\delta}$ modes excited by new composite aperture," *IEEE Trans. Antennas Propag.*, vol. 63, no. 1, pp. 433–438, Jan. 2015.
[15] X. Fang, K. W. Leung, and E. H. Lim, "Singly-fed dual-band circularly polarized dielectric resonator antenna," *IEEE Antennas Wireless Propag. Lett.*, vol. 13, pp. 995–998, May 2014.
[16] M. Zhang, B. Li, and X. Lv, "Cross-slot-coupled wide dual-band circularly polarized rectangular dielectric resonator antenna," *IEEE Antennas Wireless Propag. Lett.*, vol. 13, pp. 532–535, Mar. 2014.
[17] X.-C. Wang, L. Sun, X.-L. Lu, S. Liang, and W.-Z. Lu, "Single-feed dual-band circularly polarized dielectric resonator antenna for CNSS applications," *IEEE Trans. Antennas Propag.*, vol. 65, no. 8, pp. 4283–4287, Aug. 2017.
[18] A. Sharma, G. Das, S. Gupta, and R. K. Gangwar, "Quad-band quad-sense circularly polarized dielectric resonator antenna for GPS/CNSS/WLAN/WiMAX applications," *IEEE Antennas Wireless Propag. Lett.*, vol. 19, no. 3, pp. 403–407, Mar. 2020.
[19] I. K. C. Lin, M. H. Jamaluddin, A. Awang, R. Selvaraju, M. H. Dahri, L. C. Yen, and H. A. Rahim, "A triple band hybrid MIMO rectangular dielectric resonator antenna for LTE applications," *IEEE Access*, vol. 7, pp. 122900–122913, Aug. 2019.
[20] R. F. Harrington, *Time-Harmonic Electromagnetic Fields*. New York, NY, USA: McGraw-Hill, 1961.
[21] A. Petosa, N. Simons, R. Siushansian, A. Ittipiboon, and M. Cuhaci, "Design and analysis of multisegment dielectric resonator antennas," *IEEE Trans. Antennas Propag.*, vol. 48, no. 5, pp. 738–742, May 2000.
[22] R. T. Long, R. J. Dorris, S. A. Long, M. A. Khayat, and J. T. Williams, "Use of parasitic strip to produce circular polarisation and increased bandwidth for cylindrical dielectric resonator antenna," *Electron. Lett.*, vol. 37, no. 7, pp. 406–408, Mar. 2001.

ASMAA I. AFIFI (Student Member, IEEE) received the B.S. degree in electrical engineering from Al-Azhar University, Egypt, in 2012, and the M.S. degree in electronics and communications engineering from the Egypt-Japan University of Science and Technology (E-JUST), Alexandria, Egypt, in 2017, where she is currently pursuing the Ph.D. degree in electronics engineering with the School of Electronics, Communications, and Computer Engineering. From 2013 to 2017, she was a Research Assistant with the Microstrip Circuits Department, Electronics Research Institute, Egypt. She is currently an Assistant Researcher with the Electronics Research Institute. Her research interests include planar antennas, DRA antennas, MIMO antennas, and sensors design for breast cancer detection.

ADEL B. ABDEL-RAHMAN was born in Aswan, Egypt. He received the B.S. and M.S. degrees in electrical engineering, communication, and electronics from Assiut University, Egypt, and the Dr.-Ing. degree in communication engineering from Otto von Guericke University, Germany, in 2005. Since October 2006, he has been an Assistant Professor with the Electrical Engineering Department, South Valley University, Qena, Egypt, where he was the Executive Director of information and communication technology, from 2010 to 2012. Since October 2012, he has been with the School of Electronics, Communications and Computer Engineering, Egypt-Japan University of Science and Technology (E-JUST), Alexandria, Egypt. He was the Dean of the Faculty of Computers and Information, South Valley University, from 2016 to 2018. He is currently a Professor with the Department of Electronics and Communications Engineering, Egypt-Japan University of Science and Technology. He has published more than 120 refereed journal and conference papers. He has two patents. He also holds one patent (DE10322803A1) and one book (ISBN: 978-981-13-8047-1). His research interests include the design and analysis of antennas, filters, millimeter-wave devices, WPT, and metamaterials and their application in wireless communication, as well as optimization techniques with applications to microwave devices and antenna arrays.

ANWER S. ABD EL-HAMEED (Member, IEEE) received the B.Sc. and M.Sc. degrees from Al-Azhar University and Cairo University, Egypt, in 2009 and 2014, respectively, and the Ph.D. from the Egypt-Japan University of Science and Technology, Egypt, in May 2018, all in electronics and communication engineering. He has been with the Microstrip Circuits Department, Electronics Research Institute, Giza, Egypt, since 2010 (On leave now). He jointed Kyushu University, Fukuoka, Japan, as a special Research Student as a part of his Ph.D. program, in June 2017. He is currently a Postdoctoral Research Fellow with the Center for Northeast Asian Studies, Tohoku University, Sendai, Japan, since January 2019. His research interests include planar antennas, on-chip antennas, mm wave circuits, WPT, metamaterials, microwave imaging, and archeological survey based on electromagnetic waves. Another research interest focuses on developing radar systems for cultural heritage preservation and ground surface disaster prevention.

AHMED ALLAM received the B.Sc. degree in electrical engineering from Alexandria University, Alexandria, Egypt, and the M.Eng. and Ph.D. degrees from the University of Alberta, Edmonton, AB, Canada. From April 1994 to January 1998, he was an Instrument Engineer with Schlumberger. From May 2000 to September 2001, he was with Murandi Communications Ltd., Calgary, AB, where he worked on RF transceivers design. From April 2007 to April 2008, he worked on RF CMOS transceivers design with Scanimetrics Inc., Edmonton. He is currently an Associate Professor with the Department of Electronics and Communications Engineering, Egypt-Japan University of Science and Technology, Alexandria, Egypt. His research interest includes the design of RF circuits and systems.

SABAH M. AHMED was born in Assiut, Egypt, in 1956. She received the B.Sc. (E.E.) (Hons.) and M.Sc. (E.E.) degrees in electrical engineering from Assiut University, Egypt, in 1979 and 1985, respectively, and the Ph.D. degree from the Technical University of Budapest, Hungry, in 1992. She has worked at the Faculty of Engineering, Assiut University, as a Demonstrator, in 1979, an Assistant Lecturer, in 1985, an Assistant Professor, in 1992, an Associate Professor, in 2002, and a Professor, in 2009. She joined the Electronics Engineering Department, Hijjawi Faculty for Engineering Technology, Yarmouk University, Jordan, in 1996; Jarash Private University, Jordan, in 1997; and Computer Science Department, Zarka Private University, Jordan, in 2000, as a Visiting Professor. She has been a Professor with the Mechatronics and Robotics Engineering Department, School of Innovative Design Engineering, E-Just, Egypt, Since August 2017. Her research interests include speech analysis and synthesis, digital filters, biomedical signal processing, data compression, wavelet-transforms, genetic and immune algorithms, and mechatronics and robotics. She authored and coauthored over 60 published articles in the above fields.